Spectroscopic properties of $^3P_1$ and $^3P_0$ excited states of Bi^{3+} ions in germanate glass

Georges Boulon, Bernard Moine, and Jean-Claude Bourcet
E. R. No. 10 du Centre National de la Recherche Scientifique Laboratoire de Spectroscopie et de Luminescence
Université Claude Bernard - Lyon I - 43 Bd du 11 Novembre 1918
69622 Villeurbanne Cedex I - France
(Received 20 August 1979)

Laser-induced-fluorescence-band-narrowing and time-resolved-spectroscopy techniques are extended to measure the inequivalent sites in the spectroscopic properties of $^3P_1$ and $^3P_0$ excited states of the Bi^{3+} ion in germanate glass. Under excitation of the $^3P_1$ components, at 4 K, the analysis of the $^3P_0 \rightarrow {}^1S_0$ unsplit fluorescence band is particularly useful to probe the large site-to-site variations in the glass. The spectral dependence of the lifetime, the temporal evolution of the bandwidth under laser excitation, the red shift of both $^3P_1 \rightleftarrows {}^1S_0$ and $^3P_0 \rightarrow {}^1S_0$ transitions and the strong intensity of the forbidden $^3P_0 \rightarrow {}^1S_0$ transition are discussed. These experiments measure, indeed, the degree of inhomogeneity of Bi^{3+}-doped germanate with a broadband ion for the first time.

I. INTRODUCTION

It is well known that the optical properties of rare-earth ions in a disordered host such as a glass are very inhomogeneous. Laser-induced-fluorescence-line narrowing of rare earths in glass was first reported for Nd^{3+} (Ref. 1) and Eu^{3+} (Ref. 2). A review of this new technique applied in glasses was presented in Ref. 3.

The inhomogeneous broadening is due to site-to-site variations in the strengths of the local crystal field, electrostatic, spin-orbit interactions, and ion-phonon coupling which result in large differences in the energy levels and their radiative and nonradiative transition probabilities. Among the luminescent centers, the rare-earth ion Eu^{3+} has been useful because of its simple energy-level scheme; i.e., the first excited state, $^5D_0$, and the ground state, $^7F_0$, are singlet states. So, the $^5D_0 \rightleftarrows {}^7F_0$ transition of the particular site in which a Eu^{3+} ion sits is not split, allowing studies of inhomogeneous and homogeneous linewidths as well as the energy transfer between ions involving spectral and spatial properties.

Under broadband excitation, large inhomogeneous optical absorption and emission linewidths are observed, and nonsingle-exponential fluorescence decay occurs.

With the aid of tunable narrow-band lasers it is possible to excite only subsets of ions which are resonant with the lasing frequency. So, the fluorescence linewidths are narrower than the inhomogeneous width, and, if the lasing frequency is changed, the physical parameters describing the different local environments can be probed.

With the Eu^{3+} ion, we observe both the $^5D_0 \rightarrow {}^7F_0$ resonant transition case and the nonresonant transition case after excitation of the $^5D_1$ state.[4]

In this paper we report the details of the time-resolved laser-induced-fluorescence-band-narrowing techniques applied to the $^3P_1$, $^3P_0$, $^1S_0$ three-level scheme of the Bi^{3+} heavy ion in germanate glass. The $^3P_0 \rightarrow {}^1S_0$ transition observed under $^3P_1$ excitation is analogous to the Eu^{3+} $^5D_0 \rightarrow {}^7F_0$ nonresonant transition under $^5D_1$ excitation. We report here only our investigations of the broadband fluorescence found in the heavy-ion system.

II. Bi^{3+} SPECTROSCOPY

We have already published the absorption and emission mechanisms of the Bi^{3+} ion in crystals[5] and in germanate glass.[6] In Ref. 6, the temperature dependence of the broadband maximum shows clearly that below the theoretical thermalization temperature, $T_{th} = 50$ K, we observe only the $^3P_0 \rightarrow {}^1S_0$ transition under excitation of one of the $^3P_1$ components with a nitrogen laser. T_{th} is the temperature for which the number of photons emitted by the $^3P_1$ component is equal to the number of photons emitted by the $^3P_0$ level. Indeed, the three-level scheme on the right of the Fig. 1 is inadequate, and we must rather draw the configurational coordinate model where we assume that the vibrational potential is given by a harmonic-oscillator parabola (at left in Fig. 1). In the semiclassical Franck-Condon approximation, the absorption transition occurs from the bottom of the $^1S_0$ ground-electronic-state parabola on a vertical transition to the $^3P_1$ excited-state parabola. At liquid-helium temperature when the ion is raised to some vibrational level of the $^3P_1$ excited-state component, it quickly decays by multiphonon emis-

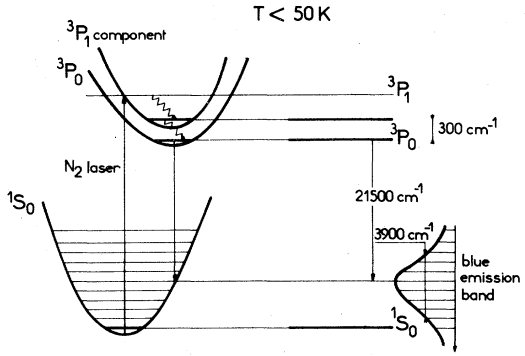

FIG. 1. The configurational coordinate model used to interpret the absorption and emission processes for the Bi^{3+} center. We have drawn only one of the three components of the $^3P_1$ state. The horizontal lines represent the vibrational levels in each electronic state. 3900 cm^{-1} is the narrowest bandwidth observed in this study (0.8% and 0.1% Bi).

sion to the ground vibrational level of the $^3P_0$ metastable level (the energy difference between the lowest vibrational levels of $^3P_1$ and $^3P_0$ state is about 300 cm^{-1} in germanate glass[6]). After the radiative decay occurs, the system ends up on some vibrational levels of the $^1S_0$ ground state. The blue emission band seen in germanate has the structure given by the vibrational levels of this ground state, because $^1S_0$ and $^3P_0$ are not split by the crystal field. On the other hand, only one decay is recorded at 4 K when we describe, as in Fig. 1, the processes at one Bi^{3+} site. This decay time τ allows us easily to determine the radiative emission probability ($A = 1/\tau$). Usually in glass we do not see the zero-phonon line because the Huang-Rhys parameter is large and the lateral displacement between $^1S_0$ and $^3P_0$ state parabolas is large. So we expect a Gaussian shape of the absorption- and emission-band envelopes.

The block diagram of the experimental apparatus used to record the time-resolved spectra was presented in Ref. 7, but now we use an IN-90 Intertechnique multichannel analyzer and photon-counting techniques to analyze the profile of the decays.

III. EXPERIMENTAL RESULTS

The fluorescence decay observed following broadband excitation into the $^3P_1$ components with a pulsed xenon lamp is nonexponential and is probably a combination of different exponential decays. Using selective laser excitation, the decay becomes more exponential and changes with the emission wavelength. If we select a very narrow spectral range (roughly 5 Å) in the wide fluorescence spectrum between 4100 and 5600 Å, at any fluorescence wavelength the decay is nearly exponential under pulsed nitrogen laser excitation. In fact the best exponential profile is observed at the long-wavelength side beyond 5200 Å (Fig. 2). Assuming an exponential decay time τ at long time, we find a very important spectral dependence between violet and yellow sites. One sees, in Fig. 3, that τ increases from 500 μs to 1 ms as the emission wavelength increases. So, the $^3P_0$ state radiative-emission probability is decreasing from 2×10^3 to 10^3 s^{-1} in the same range, a factor of 2.

Time-resolved spectroscopy experiments show unambiguously a very large variation of the $^3P_0 \rightarrow {}^1S_0$ emission-band maximum from 4400 at short time to 5400 Å at long time when exciting with the pulsed nitrogen laser. Figure 4 points out that the variation of the fluorescence-band maximum is continuous between these two limits and it explains the nonexponential decay of the integrated band intensity. On the other hand, if we plot the intensity versus wave number, after initial corrections, at any delay the emission band is Gaussian to very good approximation and the half-bandwidth increases with increasing time (Fig. 5).

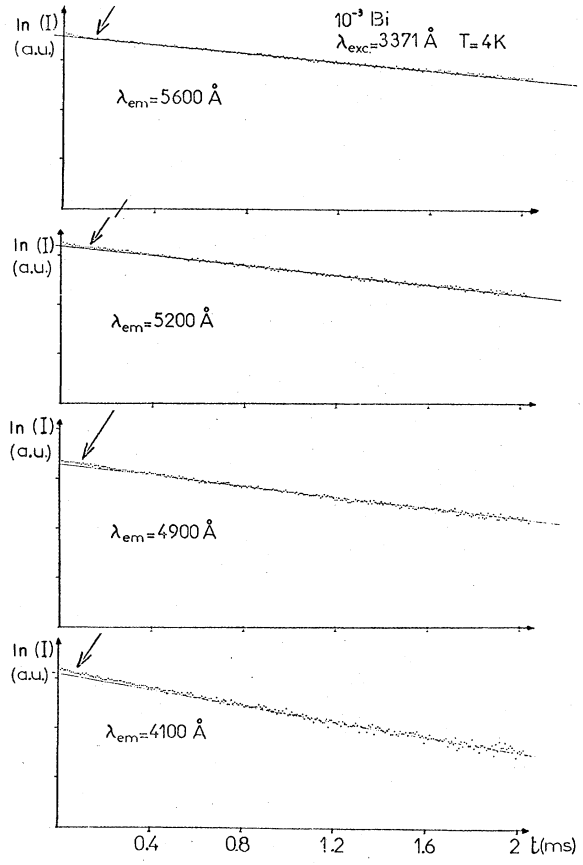

FIG. 2. Decay of the $^3P_0$ in several narrow spectral ranges (5 Å) from 4100 and 5600 Å under nitrogen-laser excitation. The time scale is the same (ms) for each decay. At left, the logarithmic intensity scale is in arbitrary units. The arrows show the discrepancy at short time between the experimental data and the exponential decay indicated by a solid line.

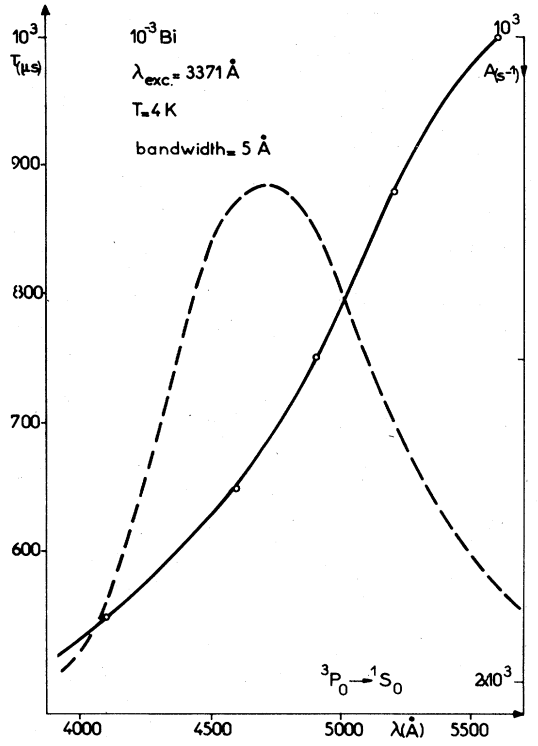

FIG. 3. Spectral dependence of the $^3P_0 \rightarrow {}^1S_0$ lifetime τ at long time: at right, τ in μs; at left, radiative emission probability in $s^{-1}(A = 1/\tau)$. The dashed curve shows the intensity of the $^3P_0 \rightarrow {}^1S_0$ fluorescence band in arbitrary units.

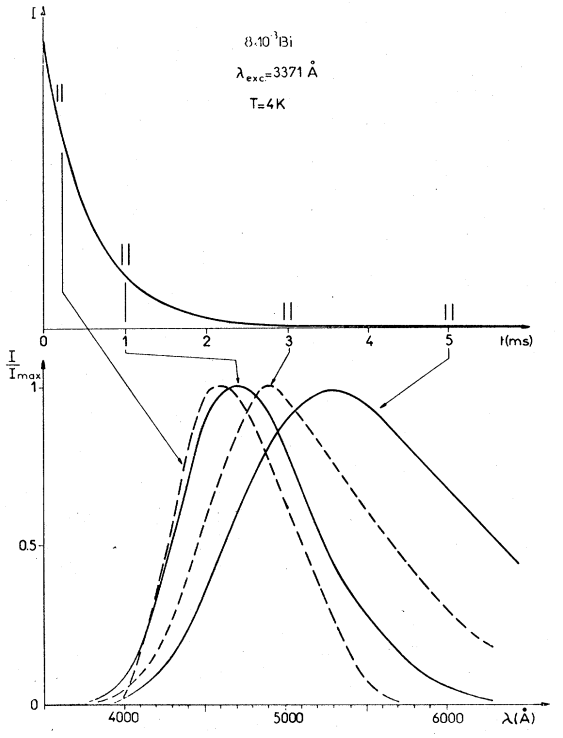

FIG. 4. Time-resolved spectra for the $^3P_0 \rightarrow {}^1S_0$ transition with nitrogen laser excitation. The arrows show the correspondence between the delay time of the boxcar integrator and the fluorescence band observed. The gate width was 100 ns.

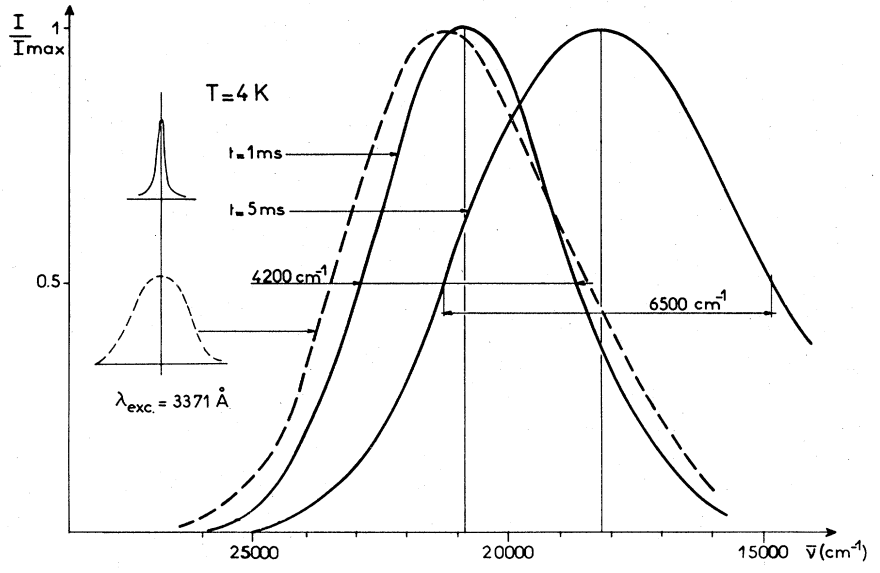

FIG. 5. The emission bands vs wave number: under nitrogen-laser excitation (solid line) at 1 and 5 ms after the pulse, and under broadband excitation given by a xenon lamp (dashed line). The intensity, in arbitrary units, is the same for the three spectra. The details of the broadening are listed in Table I.

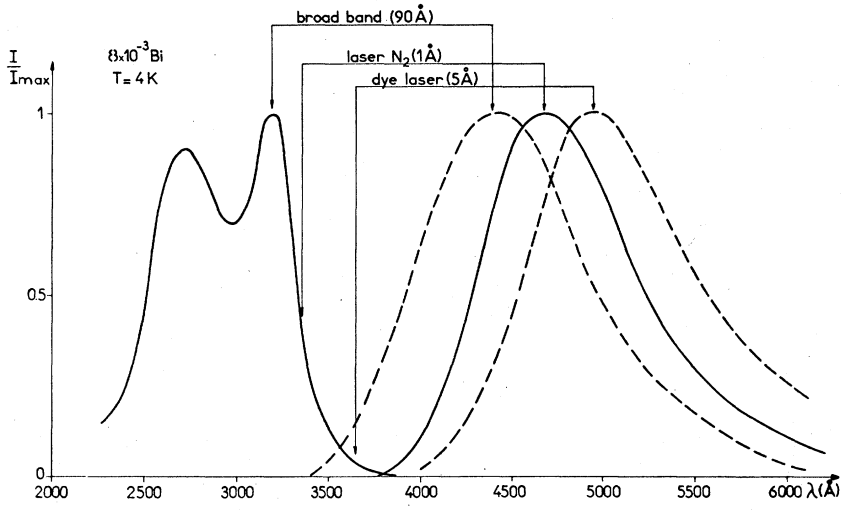

FIG. 6. The selective excitation into the $^3P_1$ state is shown by the vertical arrows on the excitation spectrum (at left). At right we see the corresponding fluorescence spectra. Vertical scale uses arbitrary units.

Table I indicates some results for two glass samples. Moreover we see that the half-bandwidth increases with the bismuth concentration.

Finally, in addition to the nitrogen laser excitation (with a half-width of 1 Å) at 3371 Å, we have also selectively excited the Bi^{3+} ion first, with a broadband xenon lamp pump (half-width of 90 Å) at 3370 Å and at the excitation spectra maximum 3190 Å, and second, with a PBD dye laser (half-width of 5 Å) at 3650 Å in the extreme low-energy side of the $^3P_1$ pump band where the excitation intensity is very weak.

The vertical arrows of Fig. 6 indicate the correspondence between the excitation line and the emission-band maximum. Two things can be noted: the fluorescence-band maximum is increasing when the excitation wavelength is increasing and the half-bandwidth is larger with the broadband pump (half-width of 5350 cm^{-1}) than with the nitrogen laser (4500 cm^{-1}) and dye-laser (3900 cm^{-1}), respectively.

TABLE I.

Concentration	Delay (ms)	Half-bandwidth (cm^{-1})
0.1% Bi	0.5	3950
	1	4000
	3	4900
	5	6300
0.8% Bi	0.01	3900
	1	4200
	3	5300
	5	6500

IV. DISCUSSION

A. Energy levels

All these experimental results are compatible with the existence of a quasicontinuum of different sites in germanate glass. Thus we propose the simple model given in Fig. 7 to explain the spectroscopic properties of the $^3P_0$ state of Bi^{3+} ion. The relative energies of the $^3P_0$ and $^3P_1$ components are shown for several Bi^{3+} ions in dissimilar sites. Because the excitation spectra are unresolved, we do not know the splittings of the $^3P_1$ state but we know the energy difference ϵ between $^3P_0$ and the $^3P_1$ lowest component for two subsets of ions: $\epsilon = 34$ meV at 4650 Å, the maximum of the emission band, and $\epsilon = 39$ meV at 5100 Å[6] on the low-energy side of the band. So, ϵ increases when the energy of the $^3P_0$ state decreases and we can conclude that the splittings between the excited states increase in magnitude from left to right. From left to right in Fig. 7 the energy of the levels move from high energy, the $^3P_0 \rightarrow {}^1S_0$ transition maximum being 4400 Å, to low energy where the $^3P_0 \rightarrow {}^1S_0$ transition maximum is 5400 Å. Radiative decay is represented by a vertical arrow. Obviously, the model described is very schematic and each ion should be drawn with the aid of the configurational curves as in Fig. 1.

The large variation in energy of the $^3P_0 \rightarrow {}^1S_0$ transition in germanate is particularly important: about 4200 cm^{-1} from this study. This is a very large range for a fluorescent center in a glass. Under excitation into $^5D_1$ states of the Eu^{3+} ion, the $^5D_0$ set of levels move only roughly 200 cm^{-1} in energy.[4] This large difference is due to the nature of the transition: the transitions between ^5D and ^7F multiplets of the Eu^{3+} rare-earth ion correspond mainly to intra $4f^6$ shell

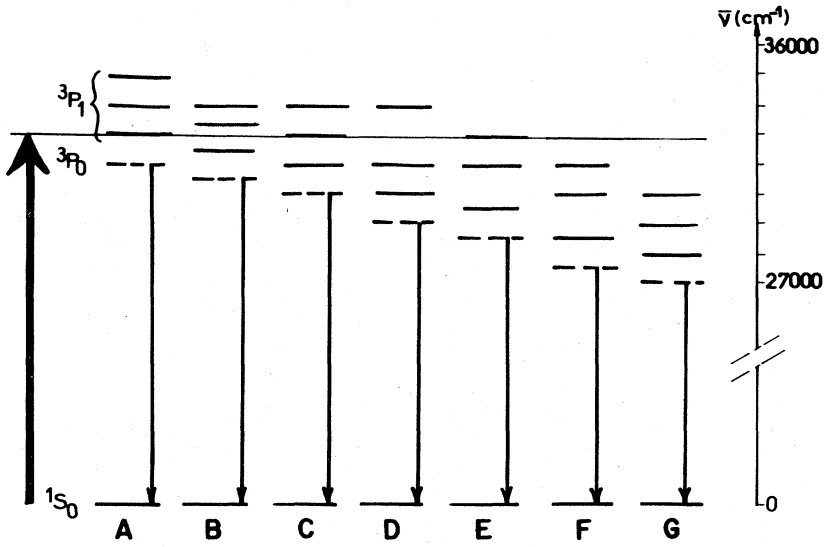

FIG. 7. The energy-level scheme of the Bi^{3+} ion distribution in germanate glass. We represent some subsets of ions from *A* to *G* sites. The vertical arrow, at left, represents the selective narrow laser excitation in resonance via three different components of $^3P_1$ state (*A*,*C*,*E* sites). After nonradiative relaxation from $^3P_1$ to $^3P_0$ levels we denote the fluorescence band by the vertical line.

transitions whereas the transitions between $6s^2$ and $6s6p$ configurations of the Bi^{3+} ion are directly influenced by the ligand orbitals.

Although the homogeneous width of this transition is probably broader than the laser width, we do not excite one site but a small subset of ions having similar spectroscopic properties due to the spectral overlap of components (the decay is nearly exponential and the shape of the emission band is Gaussian at any delay after the pulse). But we must mention that all the $^3P_1$ and $^3P_0$ excited states of these subset of ions are decreasing in energy as we see it in Fig. 7. In Fig. 7 we represent different kinds of subsets of ions which are in resonance with the laser via the three components of the $^3P_1$ state (*A*, *C*, and *E* schemes). We have also drawn some subsets of ions like *B*, *D*, *F*, and *G* for which the nitrogen laser excites some vibrational levels of each component (see Fig. 1). The distribution of the sites is not constant; its density is greatest for the subset of ions which has the highest component near 3200 Å to the left of Fig. 7 and the smallest density corresponds to ions to the right of this figure which are excited by 3650-Å radiation.

B. Fluorescence decay

We have seen that at the high-energy side, the $^3P_0 \rightarrow {}^1S_0$ transition is more allowed ($A = 2 \times 10^3\ s^{-1}$ for *A* site) than at the lower-energy side ($A = 10^3\ s^{-1}$ for *G* site). We also find a similar result with rare-earth systems where a difference factor of 2 or 3 in radiative decay rates is observed.[2] In a silicate glass variations of nearly 5 in the $^5D_0 \rightarrow {}^7F_0$ transition lifetime are noted, too.[8]

The changes in the radiative transition probabilities could reflect the changes in the refractive index *n* of the glass phases occupied by the Bi^{3+} ion. Indeed, the natural lifetime (τ_{nat}) and, then, the radiative transition probability of the $^3P_0 (A = 1/\tau_{nat})$ are given by the equation in the case where the Stokes shift between the absorption and the emission is large[9]:

$$A = \frac{1}{\tau_{nat}} = 2.88 \times 10^{-9} n^2 \langle \nu_f^{-3} \rangle_{av}^{-1} \frac{g_f}{g_u} \int \frac{\epsilon(\nu)\, d\nu}{\nu}$$

n is the refractive index, ν_f is the frequency of the fluorescence maxima, g_f and g_u are the degeneracies in the upper and lower states, and $\epsilon(\nu)$ is the molar absorptivity as a function of wave number. Unfortunately, the formula cannot be applied to the $^1S_0 \rightarrow {}^3P_0$ transition because its absorption cannot be measured because it overlaps the high intrinsic absorption of the germanate matrix and the tail of the high oscillator strength $^1S_0 \rightarrow {}^3P_1$ transition. For example, in single-crystal CaO(Bi^{3+}) the $^3P_1$ state has an allowed electric dipole transition, oscillator strength 7×10^{-3}, to the ground state[10] and the $^3P_0$ state has an oscillator strength of the order 10^{-7} to the ground state.[11]

In addition to the effect of the refractive index, we think that the large difference in decay rate could also be due to the different sites having different degrees of mixing between $^3P_1$ and $^3P_0$ levels. In CaO(Bi) and CaO(Pb) it has been concluded that the main reason for the observation of strongly forbidden tran-

sitions like $^3A_{1u}(^3P_0) \rightarrow A_{1g}(^1S_0)$ is the mixing of the $^3T_{1u}(^3P_1)$ and $^3A_{1u}(^3P_0)$ electronic states by the T_{1g} vibrations. This conclusion is true for alkali-earth sulphides as well as for alkali-earth oxides in spite of a large difference in their degree of ionicity.[12] Consequently, the radiative-emission-probability variation may measure the variation of the strong electron-phonon interaction in the glass.

C. Bandwidths

We know that an excited state like $^5D_0(Eu^{3+})$ with a lifetime of about 1 ms should give rise to a homogeneous linewidth of 10^{-8} cm^{-1}. So, the large linewidth ($\lesssim 1$ cm^{-1}) obtained with this ion is due both to the high rate of the phase-interrupting processes and the large ion-phonon coupling.[13] The lifetime of the $^3P_0$ metastable state is about 1 ms too, but the bandwidth is larger: the narrowest band obtained in this study has a 3900 cm^{-1} half-bandwidth under dye-laser excitation whereas the half-bandwidth under the broadband pump is 5350 cm^{-1}. This smallest value corresponds both to G sites in Fig. 7 and to the bandwidth observed in the fluorescence-band narrowing experiments at short time also. We note that the value remains greater than the half-bandwidth recorded[5] in $La_2O_3(Bi)$ crystal for the $^3P_0 \rightarrow {}^1S_0$ transition (2500 cm^{-1}). Obviously, this wide fluorescence band could give an additional evidence for the strong electron-phonon interaction in the glass. However, the observed shift with time of the band maximum clearly indicates that the homogeneous bandwidth is not being observed in these experiments because we pump the broad phonon side bands of a multicomponent level (Fig. 1) which is additionally inhomogeneously broadened (Fig. 7). More, during this study it was possible to excite Bi^{3+} sites with different sources but it was not possible to excite them with the same ultraviolet tunable dye laser from 3000 to 3650 Å with a constant linewidth in order to see if inhomogeneous bandwidth varies across the different sites. Under these circumstances very little site selection is possible, and we cannot obtain some absolute information about the strength of the electron-phonon coupling as in Ref. 13 where it has been demonstrated with Eu^{3+} ions that sites absorbing at the higher energy (A site) correspond to those experiencing stronger average crystal fields and having stronger electron-phonon coupling because of the larger homogeneous linewidth.

Nevertheless, the broadening observed in the time-resolved-spectroscopy experiment (Fig. 6) could be due also to the migration processes between Bi^{3+} ions. As a matter of fact, we see in Fig. 6 a small overlap between the excitation and emission spectra for the distribution of dissimilar sites. This energy transfer could involve both spatial and spectral transfer among the lower sites near of G for slightly different sites where the $^3P_0 \rightarrow {}^1S_0$ and $^1S_0 \rightarrow {}^3P_1$ transitions have the same energy. At this moment it is difficult to separate the multisite excitation from the migration processes. We see easily the $Bi^{3+}-Eu^{3+}$ energy transfer in codoped glasses.[7]

D. Nephelauxetic effect

Although broad ranges of sites are being excited rather than just one type even by using laser excitation, the experimental results show under short-wavelength excitation into the $^3P_1$ state, for example 2800 Å (35 700 cm^{-1}), the fluorescence band is violet and the proposed scheme is the excitation of a single site, in first approximation, labeled A in Fig. 7. Under long-wavelength excitation into the $^3P_1$ state, about 3800 Å (26 300 cm^{-1}), the fluorescence band is yellow and the sites are labeled G in Fig. 7. So the red shift is clearly observed in the same material and can be connected as well with the changes in covalency as with the crystal-field variations. However, we have measured the energy difference ϵ between $^3P_0$ and $^3P_1$ lowest component at 4650 and 5100 Å: we find $\epsilon = 34$ and 39 meV, respectively, that is to say a slight difference only between the two subsets of ions. This means that the $^3P_0$ and $^3P_1$ components energy levels structure belonging to one subset of ions does not depend too much of the position of the kind of the subset of ions from A sites to G sites. Then, the site to site variation of energy levels seems due to changes in covalency rather than some other effects such as crystal-field variations.

In fact, the quasicontinuum of different sites could be interpreted in terms of variations in covalency between the Bi^{3+} ion and the nonbridging O^{2-} ions forming tetrahedra. This effect, known as nephelauxetic effect, expresses the relative decrease in Racah interelectronic parameters by mixing $6p$ and ligand orbitals. The lowering of the $6s^2-6s6p$ separation measures the degree of perturbation caused by the surrounding oxygens. The stronger the perturbation is, the stronger the colavency of the Bi^{3+}–O^{2-} bond is and the lower the $^3P_0 \rightarrow {}^1S_0$ transition is.

Jørgensen[14] has explained this effect as an expansion of the partly filled shell due to the transfer of the oxygen ligand to the central atom (Bi^{3+}). The covalency can be quantitatively expressed using the following equation for the nephelauxetic parameter

$$\beta = \frac{\sigma_{\text{free}} - \sigma}{\sigma_{\text{free}}} ,$$

where σ is the wave number of the $^1S_0 \rightarrow {}^3P_1$ absorption band corresponding to a particular subset of ions and σ_{free} is the wave number of the same transition

for the free ion (75 930 cm^{-1}).

In our material β increases from 0.53 (site A) to 0.65 (site G) and can be compared with some values calculated for the $^1S_0 \rightarrow {}^3P_1$ transition of Tl^+, Pb^{2+}, and Bi^{3+} in various hosts.[9,15] This is the strongest covalency found in this way for a glass; it means that the interaction between the distribution of Bi^{3+} and O^{2-} ions is stronger in the germanate glass than in borax or phosphate glasses.

To our knowledge, the only other nonrare-earth ion used for fluorescence-line narrowing in glass is Mo^{3+} ($4d^3$).[16] The large homogeneous width ($\sim 10^3$ cm^{-1}) of the broadband $^4T_2 \rightarrow {}^4A_2$ emission masks site to site variations in the local fields but such variations are evident from the nonexponential fluorescence decay. A slight fluorescence spectral shift with laser excitation wavelength was observed by exciting into the long-wavelength tail of the $^4A_2 \rightarrow {}^4T_2$, ^2E absorption band.[17] So, this paper reports for the first time a very large shift resulting from the distribution of the sites in one glass sample doped by a heavy ion with a strong Huang-Rhys parameter.

ACKNOWLEDGMENTS

We thank Professor R. Reisfeld of the Hebrew University of Jerusalem, Israel for preparing the glass samples used in this study. Helpful discussions with the following people are gratefully acknowledged: F. Gaume-Mahn, R. Reisfeld, and M. J. Weber.

[1]L. A. Riseberg, Phys. Rev. Lett. 28, 789 (1972); Solid State Commun. 11, 469 (1972); Phys. Rev. A 7, 671 (1973).
[2]M. J. Weber, J. A. Paisner, S. S. Sussman, W. M. Yen, L. A. Riseberg, and C. Brecher, J. Lumin. 12/13, 729 (1976).
[3]M. J. Weber, Colloq. Int. CNRS 255, 283 (1976).
[4]J. Hegarty, W. M. Yen, and M. J. Weber, Phys. Rev. B 18, 5816 (1978).
[5]G. Boulon, C. Pedrini, M. Guidoni, and C. Pannel, J. Phys. (Paris) 36, 265 (1975).
[6]G. Boulon, B. Moine, J. C. Bourcet, R. Reisfeld, and Y. Kalisky, J. Lumin. 18/19, 924 (1979).
[7]J. C. Bourcet, B. Moine, G. Boulon, R. Reisfeld, and Y. Kalisky, Chem. Phys. Lett. 61, 23 (1979).
[8]C. Brecher and L. A. Riseberg, Phys. Rev. B 13, 81 (1976).
[9]R. Reisfeld and L. Boehm, J. Non-Cryst. Solids 16, 83 (1974).
[10]A. E. Hughes and G. P. Pello, Phys. Status Solidi A 25, 437 (1974).
[11]A. E. Hughes and W. A. Runciman, J. Phys. C 2, 37 (1969).
[12]A. F. Ellervee, Phys. Status Solidi B 82, 91 (1977).
[13]W. A. El-sayed, A. Campion, and P. Avouris, J. Mol. Struct. 46, 355 (1978).
[14]C. K. Jørgensen, *Oxidation numbers and oxidation states* (Springer, Berlin, 1969).
[15]R. Reisfeld, Struct. Bonding (Berlin) 13, 53 (1973).
[16]M. J. Weber, in *Proceedings of the Seventh International Conference on Amorphous and Liquid Semiconductors, Edinburgh, 1977,* edited by W. E. Spear (Stevenson, Dundee, 1977).
[17]S. A. Brawer and W. B. White, J. Chem. Phys. 67, 2043 (1977).